


# SENP3 regulates high glucose-induced endothelial dysfunction via ROS dependent signaling

Diabetes & Vascular Disease Research  
November-December 2020: 1–9  
© The Author(s) 2020  
Article reuse guidelines:  
sagepub.com/journals-permissions  
DOI: 10.1177/1479164120970895  
journals.sagepub.com/home/dvr  


Fuheng Chen , Dongdong Ma and Aizhong Li

## Abstract

**Background:** The current study aimed to explore the role of SENP3 in endothelial cell dysfunction in a high-glucose setting. **Methods:** The gene and protein expressions of SENP3 in high-glucose cultured HAECs were examined using quantitative PCR and western blotting. The effects of SENP3 on HAEC viability, apoptosis, migration, and endothelial–monocyte adhesion were evaluated in vitro by knockdown. Moreover, a mouse streptozotocin-induced type I diabetes model was established for SENP3 expression assessment. In addition, the effects of SENP3 on ROS-related signaling pathways were investigated in high-glucose cultured HAECs.

**Results:** Significantly increased levels of SENP3 mRNA and protein were found in high-glucose cultured HAECs in a time-dependent manner. SENP3 knockdown reversed high glucose-induced HAEC viability, apoptosis, and migration reduction. SENP3 knockdown attenuated the high glucose-induced intercellular adhesion of THP-1 monocytic cells and HAECs via downregulation of ICAM-1 and VCAM-1 expression. Increased levels of SENP3, ICAM-1, and VCAM-1 expression were observed in the aorta tissue of mice with type I diabetes. Downregulation of SENP3 expression was observed in HAECs cultured with high glucose levels using the free radical scavenger N-acetyl-L-cysteine or NOX4 siRNA.

**Conclusions:** SENP3 was involved in high glucose-induced endothelial dysfunction, and ROS-dependent signaling served as the mechanism.

## Keywords

SENP3, high glucose, endothelial dysfunction, diabetes mellitus, ROS

## Introduction

Diabetes mellitus (DM) causes manifestations including chronic hyperglycemia, impaired insulin secretion or action, or both and could result in vascular complications.<sup>1</sup> Owing to the changes in lifestyle, the increased prevalence of DM and related vascular complications were found in Asian countries, including China,<sup>2</sup> which requires efficient treatment strategies.

The endothelium is a single-layer cell structure located at the interface of blood and vessels for vascular function maintenance.<sup>3</sup> Many laboratory and clinical evidences have revealed that DM-induced manifestations could result in the functional changes of the vascular endothelial, including reduced anti-atherogenic function<sup>4–6</sup>; however, the underlying mechanisms have not been fully investigated.

Small ubiquitin-related modifier (SUMO) is a ubiquitin-like SUMO system post-translational protein modification pathway that was discovered in eukaryotes,<sup>7,8</sup> and SUMO-specific peptidase enzymes (SENP 1, 2, 3, 5, 6, 7) catalyze the deSUMOylation reaction that detaches the SUMO that

binds to the lysine residue of target proteins. Previous studies reveal that SENP3 is a sentrin/SUMO2/3-specific protease and a redox-sensitive molecule belonging to the SENP family, which could accumulate in cancer cells under cellular oxidative stress.<sup>9,10</sup> A former study by Huang et al. shows that elevated SENP3 is induced by hydrogen peroxide in human endothelial cells. Moreover, increased SENP3 enhanced cell proliferation, tumorigenesis, angiogenesis, and epithelial–mesenchymal transition of cancer cells via the removal of SUMO2/3 modification.<sup>11,12</sup> Most recently, SUMOylation was reported to be involved in the pathogenesis of atherosclerosis.<sup>13</sup> However, the role of SENP3 in DM has not been investigated.

Department of Cardiology, Shanxi Provincial People's Hospital, Taiyuan, Shanxi, China

### Corresponding author:

Fuheng Chen, Department of Cardiology, Shanxi Provincial People's Hospital, Taiyuan, Shanxi 030012, China.  
Email: chenfuhengdong@163.com



Based on the above findings about dysregulated SENP3 in the vessel-related pathogenesis, we explored the role of SUMO-specific peptidase 3 (SENP3) in endothelial cell dysfunction in a high-glucose setting. We found that SENP3 was involved in high glucose-induced endothelial dysfunction and reactive oxygen species (ROS)-dependent signaling served as the mechanism. SENP3 may serve as a novel target for hindering the development of vascular disease progression during DM.

## Materials and methods

### *Ethical approval of the study protocol*

The study protocol was approved by the Institutional Animal Care and Use Committee of the People's Hospital of Shanxi province, Taiyuan, Shanxi. The study was carried out according to the international guidelines for animal experimentation.

### *Cell culture*

Human aortic endothelial cells (HAECs) were obtained from Lonza Co. Ltd. and maintained in a humid atmosphere at 37°C and 5% CO<sub>2</sub> in endothelial basal medium-2 (EBM-2) containing endothelial growth medium-2 supplements (EGM-2Single Quots Kit, Lonza, Basel, Switzerland). Human acute monocytic leukemia cell line THP-1 cells were obtained from the American Type Culture Collection (Manassas, VA, USA) and cultured in RPMI 1640 medium containing 10% fetal bovine serum (Gibco, CA, USA). HAEC at passages 4–8 were used in the present study. EBM-2 containing 25 mM D-glucose without supplements and 5 mM D-glucose + 20 mM D-mannitol (with normal 5 mM D-glucose control) was used as the high glucose condition and control. Medium changes to high glucose and control was performed when the cells were grown to 60–70% confluency.

### *Lentivirus-mediated gene knockdown*

Recombinant lentiviral particles expressing SENP3, NADPH oxidase 4 (NOX4), or corresponding control short interfering (si)RNA were provided by Hanbio Co. Ltd. (Shanghai, China). The infection was performed according to the manufacturer's instructions. HAECs with various degrees of confluency were infected with lentiviral particles in EBM-2 medium with supplements for 48 h. Simultaneously, 8 µg/mL Polybrene was added into the medium to increase infection efficiency. Effect on HAEC adherence, shape, and viability after the above treatment and off-target effects of the siRNA were not observed.

### *CCK-8 assay for cell proliferation*

HAECs at a number of  $3 \times 10^3$  cells were plated in 96-well plates in EBM-2 medium with supplements and treated

with SENP3 or control siRNA lentivirus particles. Forty-eight hours later, a cell counting kit (CCK)-8 reagent was added into the wells according to the manufacturer's instructions, and the optical density was read using a microplate reader (Molecular Devices, Sunnyvale, CA, USA).

### *TUNEL staining evaluation for cell apoptosis*

HAECs at a density of 30,000 cells/well were seeded into 24-well plates, followed by SENP3 lentivirus infection and high glucose treatment for 24 h. Cell apoptosis was assayed by TUNEL staining according to the manufacturer's instructions (Beyotime, Nantong, China).

### *Wound healing assay*

HAECs at a number of 70,000 cells/well were seeded into 12-well plates. After growth to 90% confluency, a wound was made using a sterile 200 µL pipette tip, and the floating cells were removed by washing twice using EBM-2 medium with supplements. High-glucose medium containing EBM-2 and 25 mM D-glucose was added into the wells, followed by photographing at 0 and 10 h incubation at 37°C. The wound healing assay was performed after the SENP3 lentivirus or control virus-treated HAECs. To quantify the degree of cell migration, the migrated area at 10 h was subtracted from that at 0 h.

### *Endothelial-monocyte adhesion assay*

The endothelial-monocyte adhesion was assayed using the Vybrant Cell Adhesion Assay Kit. Briefly, HAECs were seeded into 24-well plates and allowed to grow to 70–80% confluency, followed by medium replacement from EBM-2 medium with supplements to EBM-2 and 25 mM D-glucose for 12 h. Calcein AM-labeled THP-1 cells at a number of  $5 \times 10^4$  cells in the same medium was added to the above HAEC cultures and incubated at 37°C for 1 h. After the removal of the non-adherent cells and washing thrice with PBS, the plates were subjected to fluorimetry at excitation and emission wavelengths of 485 and 535 nm, respectively, for fluorescence intensity quantification. Wells containing only HAEC served as blank controls.

### *Mouse type I diabetes model*

For type I diabetes models, randomly selected 10-week-old male C57Bl/6 mice (Charles River Laboratories International, Wilmington, MA, USA) were daily administered one intraperitoneal injection (IP) of newly prepared streptozotocin (STZ) (pH 4.5 in sodium citrate buffer; 60 mg/kg body weight) for 4 days, whereas the control mice only received sodium citrate buffer. All the food was removed 4 h prior to STZ or buffer injection. Blood glucose levels were determined at 3, 5, 10, and

**Table 1.** Primer sequences.

Gene name	Forward primer (5'-3')	Reverse primer (5'-3')
SENP3	GGCAGAATAATGACAGTGAC	AGTGACACAGCTCCTTGT
ICAM-1	GGCCGGCCAGCTTATACAC	TAGACACTTGAGCTCGGGCA
VCAM-1	TCAGATTGGAGACTCAGTCATGT	ACTCCTCACCTTCCCCTC
GAPDH	CAAAGCCAGAGTCCTTCAGA	GATGGTCTTGGTCCTTAGCC

17 days after fasting for 6 h, whereas the aortas were obtained after the animals were euthanized and preserved in liquid nitrogen until total protein and mRNA extraction was performed.

### Detection of intracellular ROS

Intracellular ROS levels at the setting of high glucose with or without inhibitors or Nox4 siRNA treatment were determined by the ROS assay kit (Beyotime, Nantong, China) following the manufacturer's instructions. Briefly, the cultured cells were collected and adjusted to  $1 \times 10^6$  cells/mL, followed by the addition of DCFH-DA probe from the kit to a concentration of  $10 \mu\text{M}$ . After 20 min incubation at  $37^\circ\text{C}$  and washing thrice with cell culture buffer without serum, the cells were detected at an excitation wavelength of 488 nm and emission wavelength of 525 nm using a microplate reader (Molecular Devices, Sunnyvale, CA, USA).

### Quantitative real-time reverse transcription-polymerase chain reaction (qRT-PCR)

For RNA extraction, HAECs were directly mixed with TRIzol reagent (Invitrogen), whereas aorta tissues were prepared into powder before mixing with TRIzol. One Step SYBR® PrimeScript™ RT-PCR kit (Takara, Dalian, China) and an iQ5 Real-time PCR Detection system (Bio-Rad, Hercules, CA, USA) were used for the assay, and the expression of the glyceraldehyde 3-phosphate dehydrogenase (*GAPDH*) gene was simultaneously analyzed with samples as an internal control gene. Relative gene expression was calculated using the  $2^{-\Delta\Delta\text{CT}}$  method.<sup>14</sup> PCR primers for SENP3, intercellular adhesion molecule (ICAM)-1, vascular adhesion molecule (VCAM)-1, and GAPDH are shown in Table 1.

### Western blotting

Cellular protein from HAECs or cells in frozen aorta tissue was prepared using RIPA buffer, followed by high-speed centrifugation and bicinchoninic acid (BCA) assay for protein quantification. Sodium dodecyl sulfate (SDS)-polyacrylamide gel (PAGE) electrophoresis followed by polyvinylidenedifluoride (PVDF) membrane transfer was employed for protein separation. The membranes were

blocked with 5% non-fat milk containing PBS-Tween buffer blocking and incubated with primary monoclonal antibodies against SENP3 (Abcam, Cambridge, MA, USA), ICAM-1, VCAM-1 (Cell Signaling Technology, Cambridge, MA, USA), or internal loading control GAPDH (Santa Cruz Biotechnology, Santa Cruz, CA, USA). After incubation with horseradish peroxidase (HRP)-conjugated secondary antibodies, protein bands were developed with SuperSignal Ultra Chemiluminescent Substrate (Pierce, Rockford, IL, USA) using GE ImageQuant LAS4000mini system (GE, CA, USA).

### Statistical analysis

Statistical analysis was performed using IBM SPSS version 23.0 (SPSS, Chicago, IL, USA). Data are reported as mean  $\pm$  standard deviation (SD). Student's *t*-test or one-way analysis of variance (ANOVA) was used to determine the significance for two groups and multiple groups. A *p*-value  $< 0.05$  was considered statistically significant.

## Results

### Elevated SENP3 expression in HAECs treated with high glucose

As shown in Figure 1(a) and (b), significantly increased levels of SENP3 mRNA and protein were confirmed by qRT-PCR and western blotting in HAEC after 30 min incubation with high glucose medium, and maintained until the 8 h time point.

### Attenuated high glucose induced endothelial dysfunction after SENP3 knockdown

Owing to the observation of the increasing expression of SENP3 in HAECs, we investigated whether SENP3 exerts some functional change on the HAECs in the setting of high glucose. After confirmation of the efficient SENP3 knockdown (Figure 2(a)), we found that SENP3 knockdown reversed the effects of high glucose-induced HAEC viability reduction (Figure 2(b)) and increased apoptosis (Figure 2(c)). Moreover, SENP3 knockdown reversed the effects of high glucose-induced HAEC migration suppression (Figure 2(d)). These results indicate that SENP3 was

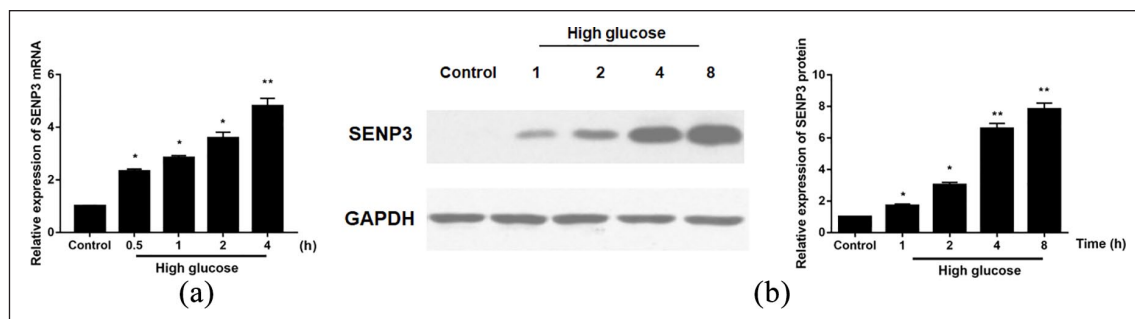


**Figure 1.** Enhanced SENP3 mRNA and protein expression in high glucose-treated HAECs: (a) at 70% confluency, HAEC was treated with EBm-2 and 25 mM d-glucose at the indicated time. SENP3 mRNA level determination by qRT-PCR and (b) SENP3 protein expression determination by western blotting.

\* $p < 0.05$ ; \*\* $p < 0.01$  versus control (normal glucose).

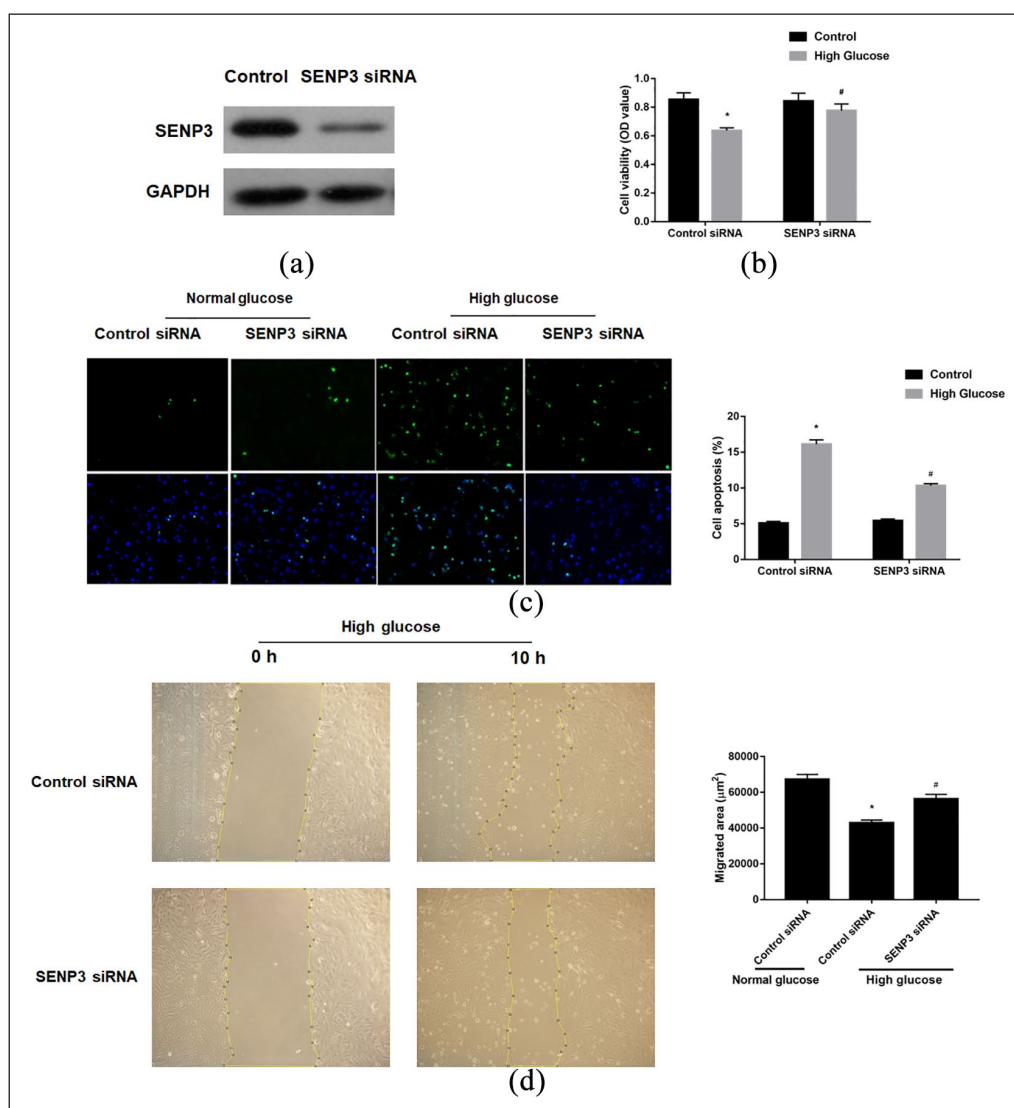


**Figure 2.** SENP3 was involved in high glucose-induced endothelial cell dysfunction: (a) the efficacy of SENP3 knockdown by siRNA was verified by western blotting, (b) high glucose-induced HAEC death was reversed by SENP3 knockdown, (c) high glucose-induced HAEC apoptosis was reversed by SENP3 knockdown, and (d) high glucose-induced HAEC migration suppression was reversed by SENP3 knockdown. All the experiments were repeated at least thrice.

\* $p < 0.05$  versus normal glucose, # $p < 0.05$  versus high glucose + control siRNA.

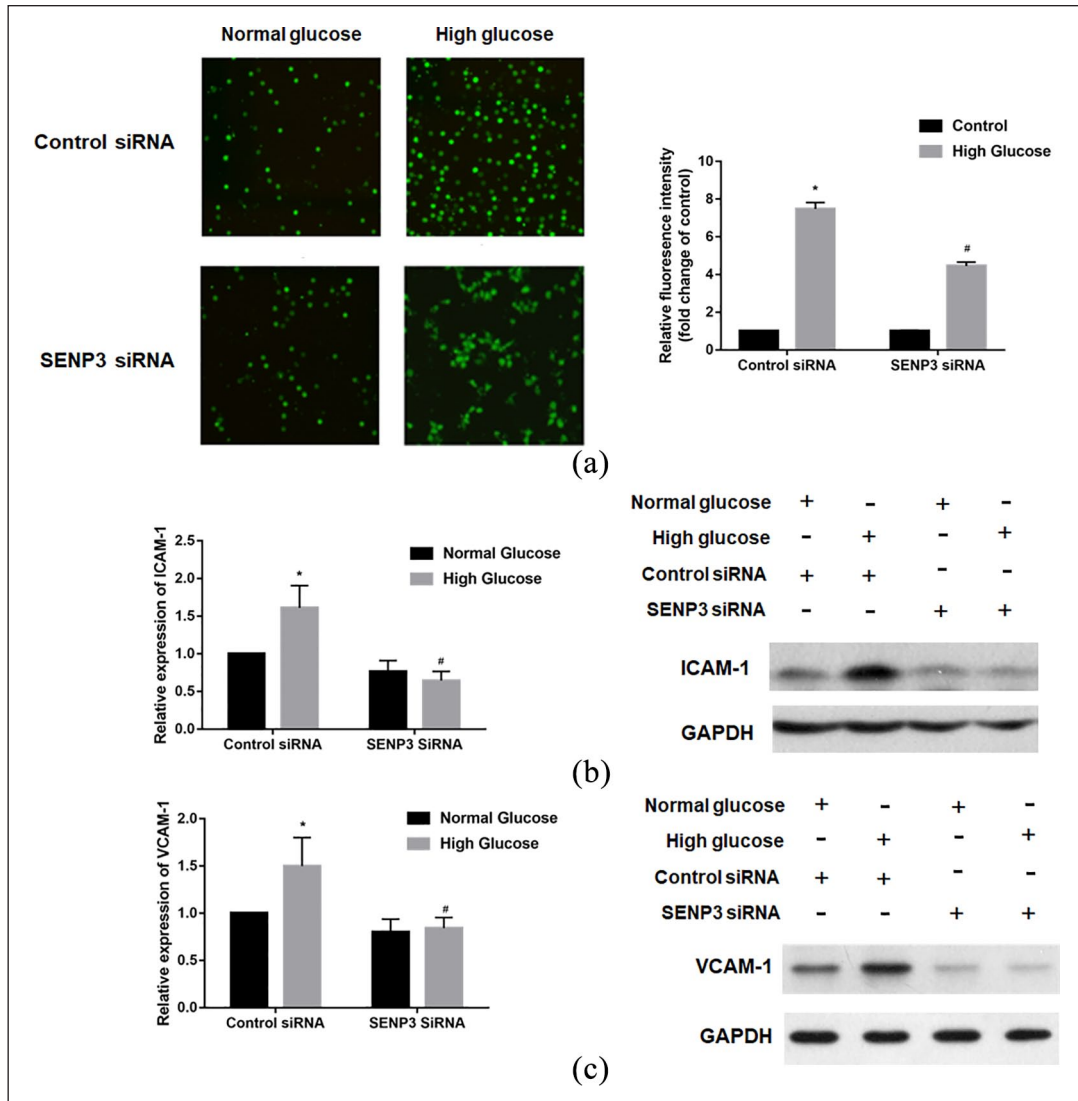


**Figure 3.** SENP3 was involved in high glucose-induced endothelial–monocyte adhesion and related adhesion molecules expression: (a) high glucose-induced endothelial–monocyte adhesion was reversed by SENP3 knockdown, (b) SENP3 was involved in high glucose-induced ICAM-1 expression, and (c) SENP3 was involved in high glucose-induced VCAM-1 expression. \* $p < 0.05$  versus normal glucose, # $p < 0.05$  versus high glucose + control siRNA.

a positive regulator in high glucose induced endothelial dysfunction.

### Attenuated high glucose induced endothelial–monocyte adhesion and adhesion molecule expression by SENP3 knockdown

Based on the above results, we further explored the role of SENP3 in the adhesion of HAECs and THP-1 monocytes. The results reveal that SENP3 knockdown significantly attenuated high glucose-induced THP-1 adhesion to HAECs (Figure 3(a)). Moreover, SENP3 knockdown significantly attenuated the expression of the adhesion molecules ICAM-1 (Figure 3(b)) and VCAM-1 (Figure 3(c)) in HAEC elevation in a high-glucose setting. Thus, these

results indicate that SENP3 is involved in high glucose induced endothelial–monocyte adhesion and related adhesion molecule expression.

### Enhanced SENP3 expression in aortas from type I diabetes mice induced by STZ

The in vitro results supported the role of SENP3 on HAECs in the setting of high glucose; therefore, we further determined the expression of SENP3 in a type I diabetes mouse model. After confirmation of the model establishment (Figure 4(a)) by a hyperglycemia statue from day 3 to day 17, we collected the mouse aorta and examined the expression of SENP3 protein. The results showed that the expression of SENP3 increased from day 3 and persisted throughout

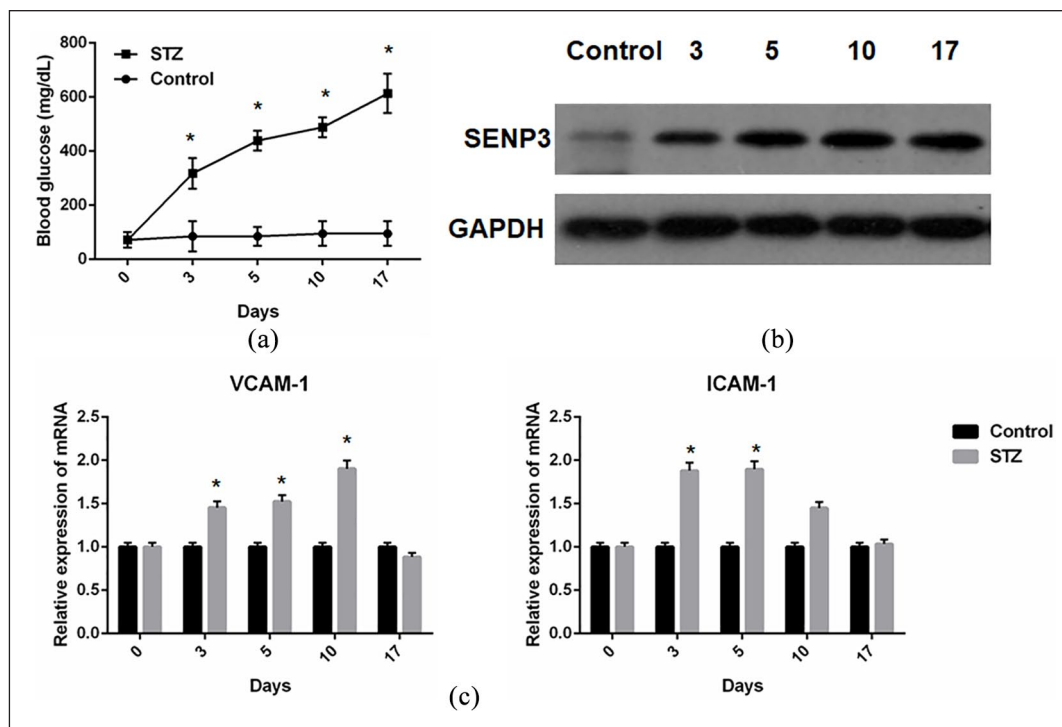


**Figure 4.** Enhanced SENP3 expression in aortas from type I diabetes mice induced by streptozotocin (STZ): (a) increased blood glucose levels after STZ administration, which confirmed the type I diabetes mice model establishment, (b) increased level of SENP3 protein expression in aortas from STZ-treated type I diabetes mice, and (c) increased level of ICAM and VCAM-1 mRNA expression in aortas from STZ-treated type I diabetes mice. \* $p < 0.05$  versus control.

the 17-day study period (Figure 4(b)). In addition, increased levels of adhesion molecules, ICAM-1 (Figure 4(c)) and VCAM-1 (Figure 4(c)), were also found in these diabetes-derived aorta tissues.

#### Reactive oxygen species were involved in enhanced SENP3 levels in HAECs induced by high glucose

We investigated the possible molecular pathways involved in high glucose-induced SENP3 expression, and the results reveal that the free radical scavenger N-acetyl-L-cysteine (NAC) decreased SENP3 expression (Figure 5(a)). After confirmation of the knockdown efficacy of NADPH oxidase 4 (NOX4) siRNA (Figure 5(b)), similar results of SENP3 expression decreasing could be found under the high glucose condition (Figure 5(c)). Moreover, high glucose-induced increase in ROS levels was suppressed by NAC or Nox4 siRNA (Figure 5(d)). The results indicate that ROS were involved in enhanced SENP3 levels in HAECs induced by high glucose.

#### Discussion

SUMOylation is ubiquitin-related transient post-translational modification pathway catalyzing the conjugation of small

ubiquitin-like modifier (SUMO) proteins (SUMO1, SUMO2, and SUMO3) to lysine residues of proteins. Previous experiments have indicated that balanced SUMOylation and deSUMOylation by SENPs are necessary for proper cardiac development (SEN1, 2, 5), metabolism (SEN1, 2), and stress adaptation (SEN1, 2, 3, 5).<sup>15</sup> Previous studies imply the engagement of SENP1-regulated SUMOylation in vasculature formation during embryonic development and severe anemia as the major cause of death in SENP1 global knockout mice, and negative SUMOylation regulation by SENP1 could result in NOTCH-related angiogenesis.<sup>16,17</sup> Moreover, Huang et al.<sup>9</sup> showed that elevated SENP3 was induced by hydrogen peroxide in human endothelial cells. Based on these insights, we demonstrated that significantly increased levels of SENP3 mRNA and protein were found in high-glucose cultured HAECs in a time-dependent manner. SENP3 knockdown reversed high glucose-induced HAEC viability, apoptosis, and migration reduction. SENP3 knockdown attenuated high glucose-induced intercellular adhesion of THP-1 monocytic cells and HAECs via the downregulation of ICAM-1 and VCAM-1 expression. Moreover, increased levels of SENP3, ICAM-1, and VCAM-1 expression were found in the aorta tissue from type I diabetes mice. In addition, the downregulation of SENP3 expression was found in high-glucose cultured HAECs using the free radical scavenger N-acetyl-L-cysteine or NOX4 siRNA.

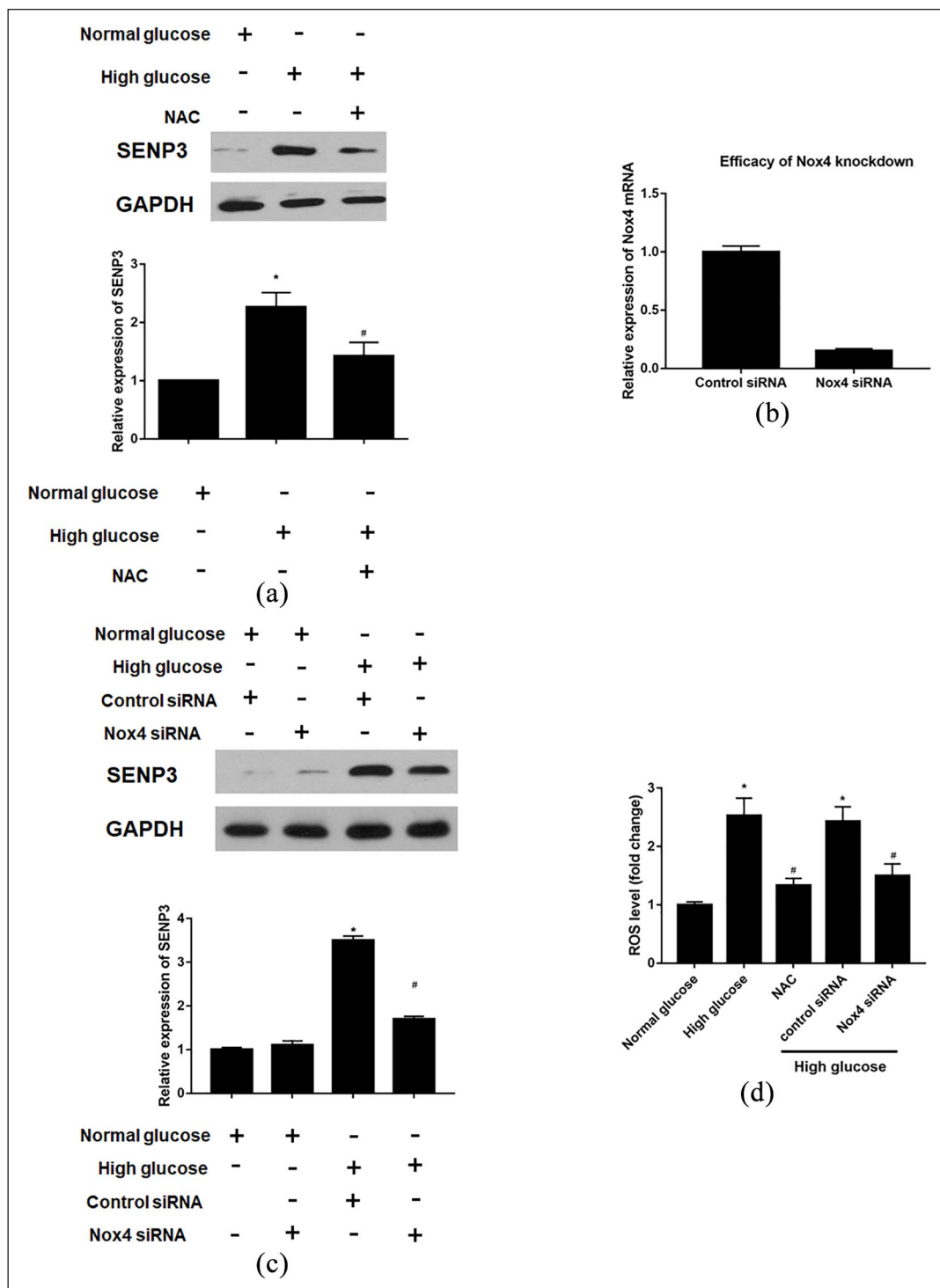


**Figure 5.** ROS related signaling is involved in the effects of SENP3 on HAECs in the setting of high glucose: (a) ROS dependent SENP3 expression in the setting of high glucose, (b) efficacy of Nox4 knockdown by siRNA, (c) decreased SENP3 level could be also achieved by Nox4 siRNA, and (d) intracellular ROS level measurement.

\* $p < 0.05$  versus normal glucose, # $p < 0.05$  versus high glucose.

In the setting of DM, the polyol pathway could be activated by chronic hyperglycemia, resulting in an increased level of advanced glycation end (AGE) products, advanced

oxidation protein products, and oxidized low-density lipoprotein (oxLDL), which could further result in the generation of the anti-oxLDL antibody.<sup>18-20</sup> High glucose levels

could increase oxidative stress, causing the dysfunction of the blood to interact with endothelial cells. Based on the above evidence of biochemical changes in the diabetes setting, we first evaluated the expression of SENP3 during high glucose conditions, and the results showed that SENP3 expression was enhanced in a time-dependent manner under high glucose conditions. The *in vitro* functional assays further identified that SENP3 knockdown could suppress high glucose-induced cell death, as illustrated by cell viability and cell apoptosis. Chronic hyperglycemia could result in angiogenesis and wound healing delay *in vivo*; therefore, we investigated whether SENP3 was involved in high glucose-induced endothelial cell migration suppression, and the results showed that SENP3 knockdown could reverse the effects of high glucose-induced cell migration suppression.

In addition to these cell behavior changes, high glucose induced an increase in oxidative stress that could increase the expression and secretion of ICAM-1 and VCAM-1, which are ligands of integrins expressed on activated monocytes, resulting in a strong adhesion of monocytes to endothelial cells and monocytes rolling on and migration into the subendothelial matrix, and even cause the development and progression of vascular diseases, such as atherosclerosis.<sup>21,22</sup> Therefore, we further evaluated the role of SENP3 on high glucose-induced adhesion molecule upregulation, and the results revealed that SENP3 knockdown significantly decreased the increase in high-glucose induced THP-1 adhesion. Moreover, SENP3 knockdown significantly attenuated the expression of adhesion molecules ICAM-1 and VCAM-1 in HAECs in high glucose settings, indicating that SENP3 was involved in the induction of adhesion molecule expression and endothelial-monocyte adhesion in the setting of high glucose.

SENP3 is a molecule preferentially located in the nucleolus, which could be continuously degraded in the nucleoplasm at the basal state. Zhou et al.<sup>23</sup> identified SENP3 as a critical positive modulator of tobacco- or cytokine-induced signal transducer and activator of transcription 3 (STAT3) activation via a previously undescribed post-translational modification-SUMOylation in head and neck cancer. In addition to STAT3, several other transcription factors (TFs) such as nuclear factor- $\kappa$ B (NF- $\kappa$ B) and promyelocytic leukemia protein (PML) could also be affected by SENP3.<sup>9</sup> These results indicate the crucial role of SENP3 in the regulation of TF activity via deSUMOylation. Moreover, SENP3 could independently regulate some of the TFs by exerting enzyme cascade activity. SENP3 could serve as a redox sensor in response to mild oxidative stress, leading to its redistribution from the nucleolus to the nucleoplasm. Thus, the increased nucleoplasmic SENP3 as an initiator could affect certain TF activity through deSUMOylation, which may play a critical role in inflammation-related diseases. For example, the expression of SUMO-2/3 induces senescence via p53- and pRB-mediated pathways, which can stimulate the

transcriptional activity of p53.<sup>24</sup> In addition, Yu et al.<sup>25</sup> found that SENP3 plays a role in the maintenance of regulatory T-cell stability and functions via BACH2 deSUMOylation, but it is also involved in the regulation of ROS-induced immune tolerance. We found that high glucose-induced SENP3 expression requires ROS-dependent signaling, as evidenced by the inhibition of the effects after treatment with the free radical scavenger NAC. Based on these results, we propose a possible signaling pathway to illustrate the events involved in SENP3-induced endothelial dysfunction by high glucose. However, the mechanism of SENP3-induced endothelial dysfunction remains unclear, and future studies should address this.

In addition, we have to declare the possible limitations of the *in vivo* data. Owing to the lack of the localization data of SENP3 in the aorta and vessel containing media and adventitia structure, the possible presence of SENP3 may not be defined in endothelial cells. Further examination of the expression and related function of SENP3 in these tissues should be performed.

## Conclusion

In conclusion, SENP3 was involved in high glucose-induced endothelial dysfunction, and ROS-dependent signaling served as the mechanism. SENP3 may serve as a novel target for hindering the development of vascular disease progression during diabetes mellitus.

## Declaration of conflicting interests

The author(s) declared no potential conflicts of interest with respect to the research, authorship, and/or publication of this article.

## Funding

The author(s) received no financial support for the research, authorship, and/or publication of this article.

## ORCID iD

Fuheng Chen  <https://orcid.org/0000-0001-8749-3159>

## References

1. American Diabetes Association. The American Diabetes Association (ADA) has been actively involved in the development and dissemination of diabetes care standards, guidelines, and related documents for many years. Introduction. *Diabetes Care* 2009; 32(Suppl. 1): S1–S2.
2. American Diabetes Association. Statistics about diabetes, <http://www.diabetes.org/diabetes-basics/statistics/> (accessed 1 March 2017).
3. Libby P. Inflammation in atherosclerosis. *Nature* 2002; 420(6917): 868–874.
4. Hadi HA and Suwaidi JA. Endothelial dysfunction in diabetes mellitus. *Vasc Health Risk Manag* 2007; 3(6): 853–876.
5. Sena CM, Pereira AM and Seica R. Endothelial dysfunction - a major mediator of diabetic vascular disease. *Biochim Biophys Acta* 2013; 1832(12): 2216–2231.



6. Avogaro A, Albiero M, Menegazzo L, et al. Endothelial dysfunction in diabetes: the role of reparatory mechanisms. *Diabetes Care* 2011; 34(Suppl. 2): S285–S290.
7. Chen Y, Sun XX, Sears RC, et al. Writing and erasing MYC ubiquitination and SUMOylation. *Genes Dis* 2019; 6(4): 359–371.
8. Yan K, Wang K and Li P. The role of post-translational modifications in cardiac hypertrophy. *J Cell Mol Med* 2019; 23(6): 3795–3807.
9. Huang C, Han Y, Wang Y, et al. SENP3 is responsible for HIF-1 transactivation under mild oxidative stress via p300 de-SUMOylation. *EMBO J* 2009; 28(18): 2748–2762.
10. Han Y, Huang C, Sun X, et al. SENP3-mediated de-conjugation of SUMO2/3 from promyelocytic leukemia is correlated with accelerated cell proliferation under mild oxidative stress. *J Biol Chem* 2010; 285(17): 12906–12915.
11. Yan S, Sun X, Xiang B, et al. Redox regulation of the stability of the SUMO protease SENP3 via interactions with CHIP and Hsp90. *EMBO J* 2010; 29(22): 3773–3786.
12. Ren YH, Liu KJ, Wang M, et al. De-SUMOylation of FOXC2 by SENP3 promotes the epithelial-mesenchymal transition in gastric cancer cells. *Oncotarget* 2014; 5(16): 7093–7104.
13. Dehnavi S, Sadeghi M, Penson PE, et al. The role of protein SUMOylation in the pathogenesis of atherosclerosis. *J Clin Med* 2019; 8(11): 1856.
14. Ji Y, Strawn TL, Grunz EA, et al. Multifaceted role of plasminogen activator inhibitor-1 in regulating early remodeling of vein bypass grafts. *Arterioscler Thromb Vasc Biol* 2011; 31(8): 1781–1787.
15. Mendler L, Braun T and Muller S. The ubiquitin-like SUMO system and heart function: from development to disease. *Circ Res* 2016; 118(1): 132–144.
16. Zhu X, Ding S, Qiu C, et al. SUMOylation negatively regulates angiogenesis by targeting endothelial NOTCH signaling. *Circ Res* 2017; 121(6): 636–649.
17. Yu L, Ji W, Zhang H, et al. SENP1-mediated GATA1 deSUMOylation is critical for definitive erythropoiesis. *J Exp Med* 2010; 207(6): 1183–1195.
18. Kalousova M, Skrha J and Zima T. Advanced glycation end-products and advanced oxidation protein products in patients with diabetes mellitus. *Physiol Res* 2002; 51(6): 597–604.
19. Martin-Gallan P, Carrascosa A, Gussinye M, et al. Biomarkers of diabetes-associated oxidative stress and antioxidant status in young diabetic patients with or without subclinical complications. *Free Radic Biol Med* 2003; 34(12): 1563–1574.
20. Boullier A, Bird DA, Chang MK, et al. Scavenger receptors, oxidized LDL, and atherosclerosis. *Ann N Y Acad Sci* 2001; 947: 214–222; discussion 222–223.
21. Izuta H, Matsunaga N, Shimazawa M, et al. Proliferative diabetic retinopathy and relations among antioxidant activity, oxidative stress, and VEGF in the vitreous body. *Mol Vis* 2010; 16: 130–136.
22. Blankenberg S, Barbaux S and Tiret L. Adhesion molecules and atherosclerosis. *Atherosclerosis* 2003; 170(2): 191–203.
23. Zhou Z, Wang M, Li J, et al. SUMOylation and SENP3 regulate STAT3 activation in head and neck cancer. *Oncogene* 2016; 35(45): 5826–5838.
24. Li T, Santockyte R, Shen R-F, et al. Expression of SUMO-2/3 induced senescence through p53- and pRB-mediated pathways. *J Biol Chem* 2006; 281(47): 36221–36227.
25. Yu X, Lao Y, Teng X-L, et al. SENP3 maintains the stability and function of regulatory T cells via BACH2 deSUMOylation. *Nat Commun* 2018; 9(1): 3157.